sustainability

MDPI

Article

Impact of Ship Emission Control Area Policies on Port Air Quality—A Case Study of Ningbo Port, China

Siling Lu [1,2] and Fan Zhou [1,2,*]

[1] College of Information Engineering, Shanghai Maritime University, Shanghai 201306, China; 202230310294@stu.shmtu.edu.cn
[2] Shanghai Engineering Research Center of Ship Exhaust Intelligent Monitoring, Shanghai 201306, China
* Correspondence: fanzhou_cv@163.com

Abstract: The implementation effectiveness of ship emission control area (ECA) policies can be effectively evaluated using econometric models. However, existing studies mainly focus on changes in SO_2 concentrations in the air. In order to comprehensively assess the impact of ECA policies on air quality, this study takes Ningbo Port in China as an example and uses a regression discontinuity (RD) model to analyze the influence of ship emissions around the wharf on concentrations of SO_2, NO_2, and particulate matter (PM) in the air. The results indicate that individual ships' activities within the monitoring area (within 300 m) make a relatively small contribution to the concentration of SO_2 in the air and do not form a significant breakpoint. However, there is a noticeable breakpoint in the concentration of NO_2 around the monitoring point as the ship approaches. At the same time, the variation range of $PM_{2.5}$ is significantly greater than that of PM_{10}, which aligns with the characteristics of PM emitted by ships. The experimental results have passed three robustness tests, demonstrating that the current policy on ship ECAs has a positive limiting effect on SO_2 emissions and, to some extent, reduces PM emissions. However, further reductions in ship emissions may require more restrictions in nitrogen oxide emissions.

Keywords: air pollution; ship emissions; emission control area; Ningbo Port

Citation: Lu, S.; Zhou, F. Impact of Ship Emission Control Area Policies on Port Air Quality—A Case Study of Ningbo Port, China. *Sustainability* **2024**, *16*, 3659. https://doi.org/10.3390/su16093659

Academic Editor: Christos Kontovas

Received: 9 April 2024
Revised: 20 April 2024
Accepted: 25 April 2024
Published: 26 April 2024

1. Introduction

Ship fuel combustion emits various air pollutants, including sulfur dioxide (SO_2), nitrogen oxides (NO_x), particulate matter (PM), and volatile organic compounds (VOCs). These pollutants contribute to the deterioration of air quality and have adverse effects on human health, such as respiratory diseases and cardiovascular disorders [1,2]. Among them, SO_2 primarily originates from the combustion of sulfur elements in fuels. When released into the atmosphere, it reacts with water molecules to form sulfuric acid, which is one of the main components of acid rain [3]. Nitrogen oxides mainly result from chemical reactions between nitrogen gas (N_2) and oxygen gas (O_2) under high temperature and pressure conditions. They not only pose risks to human health but also contribute to the formation of acid rain and photochemical smog [4]. Particulate matter can enter the respiratory system, especially fine particles like $PM_{2.5}$ that can penetrate deep into the lungs, causing respiratory inflammation, exacerbating asthma symptoms, and other respiratory diseases. VOCs react with nitrogen oxides (NO_x) under sunlight exposure to form ozone and secondary particulate matter [5].

In order to limit the harm of ship emissions on human health and the ecological environment, the International Maritime Organization (IMO) has established regulations through the International Convention for the Prevention of Pollution from Ships and its Annex VI [6]. The relevant measures were adopted in 1997 but only came into effect in 2005. The main measures include setting a global upper limit for sulfur content in ship fuel; starting from 2012, the global upper limit for fuel sulfur content (FSC) was set at

3.5% (m/m), which has been reduced to 0.5% (m/m) since 2020. IMO also established four international emission control areas (ECAs) for ships: Baltic Sea area, North Sea area, North American area, and United States Caribbean Sea area. Since 2015, the maximum FSC allowed within these ECAs is set at 0.1% (m/m) [7]. Compared with the monitoring requirements for sulfur content in fuel, the regulation of NO_x emissions is more difficult because shipping companies need to pay more costs to deal with nitrogen oxide emission reduction regulations [8], which may affect their enthusiasm for implementing emission reduction regulations. Moreover, the influencing factors of NO_x emissions are far more complex than SO_2, leading to the inability to effectively monitor NO_x emissions caused by engine deterioration or improper operation and maintenance or failure or even shutdown of exhaust gas reprocessing devices (Tier III vessels) [9,10].

Despite the implementation of international ship ECAs for nearly 20 years, the IMO has yet to establish a ECA in East Asia, where maritime traffic is most dense. China, being a major shipping nation, had a civilian fleet of 12.19×10^4 vessels and transported over 85.54×10^4 tons of goods by waterways by the end of 2022. Its national port cargo throughput reached an impressive 101.31×10^8 tons, ranking first in the world [11]. Among the top ten ports globally, seven are located in China, with Ningbo-Zhoushan Port leading in cargo throughput at 12.61×10^4 tons. In order to actively address the impact of ship emissions, China's Ministry of Transport issued the "Implementation Plan for Ship ECAs in Pearl River Delta, Yangtze River Delta and Bohai Rim (Beijing-Tianjin-Hebei) Waters" in December 2015 [12]. This plan established domestic ECAs within these three major coastal regions of China. By the end of 2018, the Ministry further upgraded and improved this plan by releasing a new implementation scheme that expanded China's ECAs to cover all coastal region and major inland river areas [13].

Since the implementation of policies related to ship ECAs, numerous scholars have conducted a series of studies to verify the positive impact of ECA policies on air quality [14–19]. Among them, econometric models have received significant attention [20]. This is because econometric models can accurately identify and estimate the causal effects of policy changes on economic variables [21]. This method helps distinguish policy effects from other interfering factors, thus providing more accurate policy evaluations. Wan et al. (2019) used a difference-in-difference (DID) model to compare and demonstrate the effectiveness of ECA policies in the Pearl River Delta, Yangtze River Delta, and Bohai Rim (Beijing-Tianjin-Hebei) [22]. Zhang et al. (2020) employed an RD model to demonstrate that the daily average concentration of SO_2 in Shanghai Port decreased by 0.229 $\mu g/m^3$ after the implementation of ECA policies in 2016 [23]. Zhou et al. (2021) evaluated the impact of ship ECA policies on sulfur dioxide concentration in port areas using a DID model [24]. Zhang et al. (2022) assessed the effectiveness of ECA policies in four major port cities in China's Yangtze River Delta region and examined heterogeneity in policy effects among different port cities within the same region [25]. Zhou et al. (2023) analyzed improvements in air quality at various stages before and after ECA policy implementation at Shanghai Port from both local and regional perspectives [26].

Overall, the implementation of ECAs policies does have quantifiable positive impacts on local and regional air quality. However, the current measures limiting FSC in ECAs contribute only limitedly to global emissions reduction demands. Cullinane and Bergqvist analyzing established international ECAs and their policy impacts, found that the effectiveness of current fuel restrictions in ECAs is quite limited in meeting global emissions reduction demands [27]. They suggest that stricter limits on sulfur oxides and nitrogen oxides emissions need to be implemented in the future, along with broader geographical coverage of such policies. Furthermore, they propose that shipping companies' development plans should integrate energy use with other energy-saving methods [28]. Therefore, this study aims to comprehensively understand the impact of ECA policies on air quality as a starting point. Based on actual air measurement results at Ningbo Port, we employ an RD model to analyze the characteristics of air quality changes during ships' arrival and

departure times, thus providing a more detailed analysis of the effects of ship emission restriction policies on port air quality.

2. Materials and Methods

Ningbo Port, located in the central part of China's mainland coastline, is situated on the southern wing of the Yangtze River Economic Belt. It serves as a crucial hub in China's comprehensive transportation system and plays a significant role as an important port for foreign trade and maritime transit. In 2022, the port handled a cargo throughput of 1261.34 million tons and container throughput of 33.51 million TEUs, representing respective year-on-year growth rates of 3.0% and 7.8% [29]. The port area is mainly used for containers, bulk dry bulk cargo, crude oil, refined oil and liquid chemicals, food and groceries transportation vessels, and cruise passenger transport.

The data used €n this study were collected from two monitoring points at Beilun wharf in Ningbo Port, as shown in Figure 1. Monitoring point 1 is located along the shore with berths to its south, while monitoring point 2 is situated on an outer breakwater with berths on both its north and south sides, closer to the shipping channel. Monitoring points 1 and 2 are located in different directions of the same wharf, with significant differences in berths. As a result, vessel activities at monitoring point 2 are more intensive compared to those at monitoring point 1. By comparing the monitoring data from these two points with varying vessel densities, a more comprehensive conclusion can be drawn regarding the impact of vessel activities on wharf air quality. The heights of monitoring point 1 and monitoring point 2 are, respectively, 20 m and 15 m. With their different orientations, the monitoring devices at both points effectively avoid structural interference. The monitoring period for this study ranged from January to March 2023, focusing on measuring concentrations of SO_2, NO_2, $PM_{2.5}$, and PM_{10} as well as wind speed and direction data. There are two main methods of measuring the smoke plume emitted from ships: the optical method and the "sniffing" method [30,31]. We employed two land-based monitoring devices based on the "sniffing" method for data collection in this study. This type of device has been tested and proven to provide consistent and reliable monitoring data in previous research [32,33].

According to the relevant policies of the China ECA policies, since 1 January 2019, ships entering the Ningbo Port Area should use Marine fuel oil with a sulfur content of no more than 0.5% (m/m). After nearly four years of policy implementation, ships are basically required to use low-sulfur fuel in accordance with regulations [34]. Based on this, the article selects concentration data of sulfur dioxide, nitrogen dioxide, and particulate matter in specific areas of the port to analyze whether there is a significant change in air quality near the port when ships emit according to regulations after implementing ECA policy. This analysis aims to evaluate if the ship emission control zone policy effectively restricts ship emissions. In order to analyze the contribution of ship emissions to wharf air quality, this paper adopts the accurate breakpoint regression model to analyze the monitoring data. This is a randomized experiment method, which can effectively solve the endogeneity problem and is the most reliable method among quasi-experimental methods, which can better identify causality [35].

The data collection frequency is one sample per second, and this paper conducts breakpoint regression analysis based on the number of ships passing through the monitoring point every hour. To facilitate comprehensive analysis, the average concentration data collected by the two monitoring stations within one hour are taken as a unit. Since the automatic identification system (AIS) of ships tracks and records ship positions using longitude and latitude, the longitude and latitude of all identified ships obtained through AIS are compared with the longitude and latitude positions of the two monitoring points based on their relative distances. The observation data are divided into two categories: the ship is docked or sailing within 300 m of the monitoring equipment, and the ship is not present. That is, the concentration data of SO_2, NO_2, $PM_{2.5}$, and PM_{10} within 1 h of the ship docking or departure appear before the breakpoint; otherwise, the data appear after the breakpoint. Since there may be multiple ships passing through the monitoring

equipment and berthing at the same time, the ascending quadratic ranking method is used to determine the influence of the number of ships on the wharf. The breakpoint regression model is constructed as follows:

$$Y_t = \alpha_0 + rD_t + \beta_1 f(x_t) + \beta_2 D_t f(x_t) + \varphi Z_t + \mu_t \quad (1)$$

Figure 1. (**a**) Relative position map of Ningbo Port and the Yangtze River; (**b**) location of the measurement station; (**c**) monitoring point 1; (**d**) monitoring point 2.

Among them, Y_t represents the average mass concentration of SO_2, NO_2, $PM_{2.5}$, and PM_{10} measured at two monitoring points in the port terminal at time t. The value of t is determined based on the number of ships and specific time points. α_0 denotes individual fixed effects, which are unobservable variables that affect Y_t at the individual level but do not change with time. When $t < 0$, it indicates that there are ships entering or leaving the port within the current hour unit, and $D_t = 0$ in this case. When $t \geq 0$, it means that there are no ships entering or leaving the port within the current hour unit, and $D_t = 1$ in this case. R represents the coefficient of treatment variable D_t, indicating the policy's disposal effect. If r is statistically significant, it implies a significant correlation between ship activities (presence or absence) and contributions to SO_2, NO_2, $PM_{2.5}$, and PM_{10} levels in port cities; if r is not statistically significant, it means that ship activities will not cause drastic changes in air quality at the wharf. This indirectly reflects that there is no difference in the concentration of pollutant gases emitted by ships when they are close to or far away from the wharf. Therefore, this indicates that ships maintain a stable emission state after entering the emission control zone, confirming the effectiveness of the policy. $f(x_t)$ refers to a polynomial function with respect to time t as a trend term; β_1 is its estimated coefficient. $D_t f(x_t)$ represents an interaction term between treatment variable and time trend term which helps better understand their joint impact on outcome variables; and β_2 is the

estimated coefficient for $D_t f(x_t)$. The related control variables Z_t represent wind direction and wind speed measured at monitoring points in the port terminal. The channel is located in the southwest direction of the berth, with monitoring point 1 on the crane inside the berth's inner channel and monitoring point 2 on the crane outside the berth's outer channel. Therefore, as both monitoring points are located in the southwest direction of the waterway, combined with the traffic situation of vessels at the wharf, when the wind direction is west or southwest (180°–270°), pollutants emitted by vessels from the direction of the waterway will be more transported to the monitoring point, and the collected pollutant concentration will be more affected by the wind condition. Therefore, 180°–270° is set as downwind direction. Φ denotes their effect coefficients. M_t stands for error terms explaining unknown contributing factors. According to monitoring data, Table 1 presents statistical values for major variables. Jan-1, Jan-2, Feb-1, Feb-2, Mar-1, and Mar-2, respectively, indicate data collected by monitoring points 1 and 2 during January, March, and February.

Table 1. Descriptive statistics of the variables.

	Variable	Obs.	Mean.	Std. Dev.	Min.	Max.
Jan-1	SO_2	610	25.331	32.896	15.72	539.982
	NO_2	610	114.884	56.919	25.568	661.196
	$PM_{2.5}$	610	61.162	38.765	0	191
	PM_{10}	610	73.104	43.312	0	227
	W-direct	610	207.877	102.748	0	334
	W-speed	610	3.300	3.079	0	13.5
	Count	610	3.839	12.211	0	68
Jan-2	SO_2	612	937.660	1323.41	18.34	5107.69
	NO_2	612	231.617	162.942	56.964	1690.87
	$PM_{2.5}$	612	56.702	35.709	2	195
	PM_{10}	612	67.482	39.010	3	213
	W-direct	612	192.701	60.062	23	323
	W-speed	612	3.935	2.828	0.4	12.3
	Count	612	34.630	24.002	0	159
Feb-1	SO_2	476	24.745	23.575	20.436	326.452
	NO_2	476	107.024	35.805	9.776	262.448
	$PM_{2.5}$	476	44.476	38.898	6	217
	PM_{10}	476	53.850	45.689	8	251
	W-direct	476	149.199	100.078	33	334
	W-speed	476	2.643	1.560	0.4	8.3
	Count	476	10.588	17.619	0	75
Feb-2	SO_2	476	786.236	1181.65	21.222	4997.38
	NO_2	476	336.429	347.921	74.448	3130.76
	$PM_{2.5}$	476	39.855	37.183	3	254
	PM_{10}	476	47.611	41.947	5	275
	W-direct	476	218.407	49.947	111	345
	W-speed	476	2.943	1.580	0.6	10.2
	Count	476	36.993	28.117	0	134
Mar-1	SO_2	375	20.110	11.121	9.956	150.65
	NO_2	375	99.318	91.535	1.692	834.532
	$PM_{2.5}$	375	39.378	33.722	0	155
	PM_{10}	375	47.224	38.545	0	171
	W-direct	375	153.944	82.651	32	336
	W-speed	375	1.702	1.360	0.2	7.3
	Count	375	3.352	6.516	0	33
Mar-2	SO_2	400	554.473	960.625	10.218	5088.30
	NO_2	400	218.740	194.321	1.88	1728.47
	$PM_{2.5}$	400	34.867	28.359	0	129
	PM_{10}	400	41.992	32.745	0	140
	W-direct	400	236.052	61.112	51	325
	W-speed	400	2.826	1.617	0.4	9.3
	Count	400	34.937	31.978	0	150

Obs. Represents the number of samples; Mean, Min, Max, and Std. dev. Represent the average value, minimum value, maximum value, and standard deviation of SO_2, NO_2, $PM_{2.5}$, and PM_{10} concentrations, respectively. W-direct and W-speed refer to wind direction and wind speed. The concentration of all pollutant gases is in units of $\mu g/m^3$, and the rest of the table below is the same.

3. Results

From Figure 1, it can be observed that only the northern side of monitoring point 1 allows for ship berthing, and it is relatively further away from the shipping channel. The measured gas concentrations at this point mainly originate from nearby moored ships. On the other hand, both sides of monitoring point 2 allow for ship berthing and are closer to the shipping channel. This results in relatively higher values of SO_2, NO_2, $PM_{2.5}$, and PM_{10} measurements at monitoring point 2 compared to monitoring point 1.

3.1. Contribution of Ship Emissions to SO_2 Concentration

The scatter plot of SO_2 concentration at two monitoring points in January, February, and March is shown in Figure 2. When conducting regression data preprocessing, the pollutant gas concentration values collected per unit hour are sorted according to the number of vessels in descending order. Before the breakpoint, the number of vessels is greater than 0, indicating that there are vessels passing through or berthing at the monitoring point of the wharf. After the breakpoint, the number of vessels is equal to 0, indicating that there are no vessels passing through the monitoring point at this time. Therefore, on the horizontal axis, it represents the serial number of pollutant gas concentration values per unit hour sorted by vessel count, while the vertical axis represents the SO_2 concentration measured at Ningbo Port monitoring point. The red solid circles represent the current serial number's SO_2 concentration, and the gray vertical lines represent breakpoints where policy changes were implemented. The left side of the gray vertical line represents units with ships entering and leaving the port per hour, while the blue curve represents fitting results before the breakpoint; on the right-side, representing units without ships entering or leaving Beilun wharf per hour, there is a green curve representing fitting results after the breakpoint. Among them, there are no obvious breakpoints in SO_2 concentrations for monitoring point 1 (Figure 2a,c,e). In March, for monitoring point 2 (Figure 2f), there are no apparent breakpoints either. However, Figure 2b,d show clear downward and upward breakpoints, respectively, except for four obvious outliers. The scatter distribution in fitted result graphs is mainly concentrated between 0 and 2000 $\mu g/m^3$; outliers may be caused by environmental factors or data collection errors from equipment. Overall, this indicates that ship emissions contribute to some extent to SO_2 levels in port air but are not significantly noticeable; significant variations can only be observed in areas with high ship density.

Further quantitative analysis was conducted to assess the contribution of ship emissions to the concentration of SO_2 in the air at the wharf. First, a breakpoint regression model was constructed to perform polynomial regressions ranging from the first to the ninth order on the SO_2 concentration. Second, wind speed and direction were included as control variables for comparison. Bayesian information criterion value (BIC) and Akaike information criterion value (AIC), two important indicators, were then used to determine the order of the polynomial function. Finally, AIC and BIC values were calculated for different orders, and the corresponding r value associated with the minimum AIC value was selected as the regression result. The polynomial regression results are shown in Table 2. To analyze the impact of wind speed and direction, models both without control variables (a) and with control variables (b) were established.

The results in Table 2 indicate that regardless of whether there are control variables considered (i.e., accounting for wind speed and direction), there is no significant correlation between ship activities at berth and SO_2 concentration for these ten sets of data from monitoring points 1 and 2 during the February–March period. This suggests that ship activities at wharfs do not have a noticeable effect on the SO_2 concentration in the air. Although there is a significant negative regression result for monitoring point two in January, this could still be attributed to individual outliers when considering Figure 2b. Additionally, higher numerical values at monitoring point 2 indicate more severe pollution near areas with dense shipping traffic. When including control variables such as wind speed and direction, it can be observed that there is not much difference in revalues among

each set of data groups. This implies that wind speed and direction have minimal influence on SO_2 concentration in dockside air.

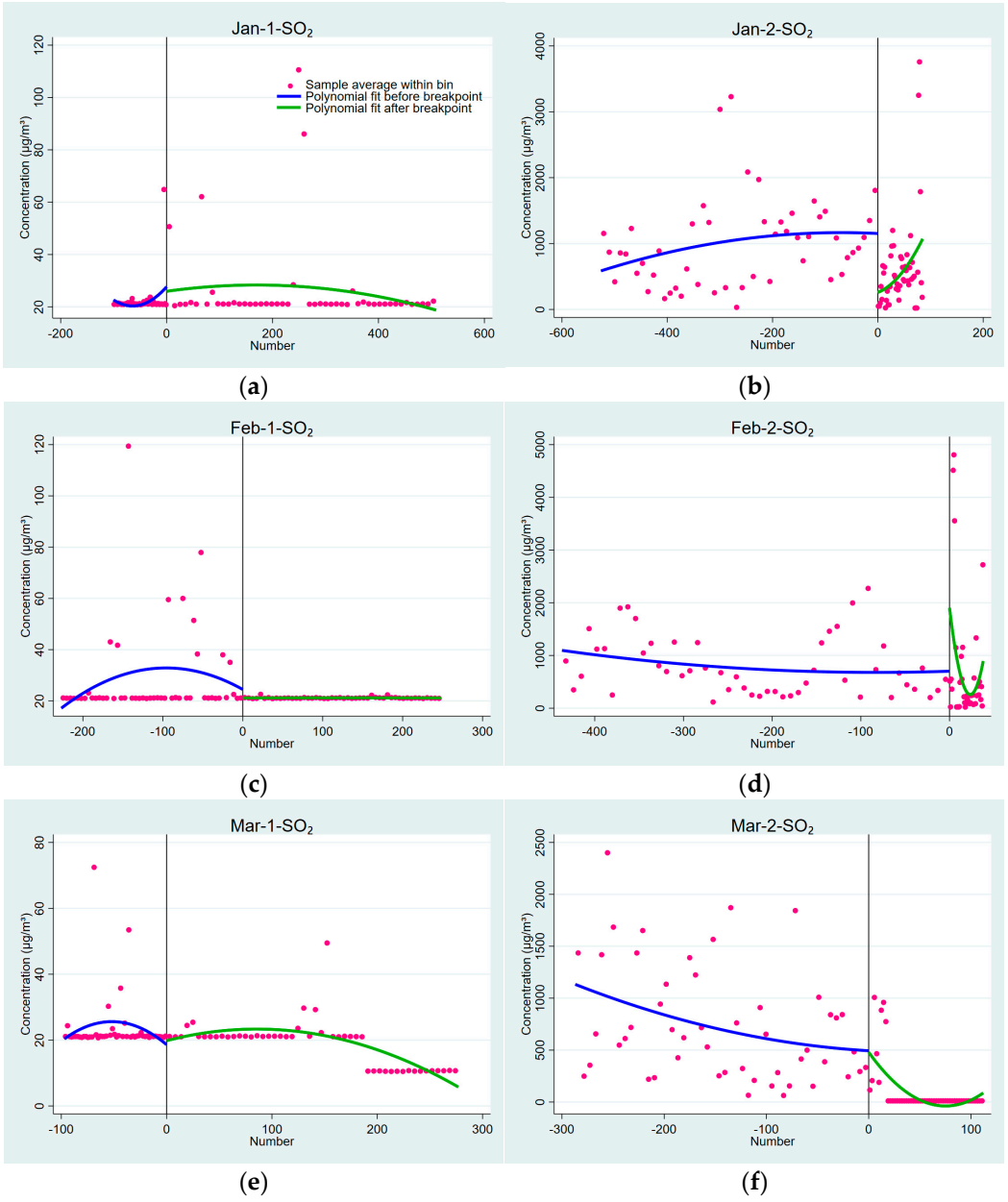

Figure 2. Hourly SO_2 concentrations for January, February, and March 2023 measured at the two monitoring stations of the Beilun Wharf. The abscissa represents the serial number of the SO_2 concentration data, arranged in chronological order. The breakpoint (grey vertical line) determines whether any ship did (<0) or did not (>0) sail within 300 m of the monitoring point within an hour. The red dots represent the average SO_2 concentration for the corresponding hour. The green and blue lines show the fit of the RD model before and after the breakpoint, respectively. Because of the large number of data points, only the average value for the corresponding time period is shown.

Table 2. Polynomial regression results of SO_2.

	Jan-1-SO_2		**Feb-1-SO_2**		**Mar-1-SO_2**	
	(a)	**(b)**	**(a)**	**(b)**	**(a)**	**(b)**
r	20.32	24.13	−3.300	−4.323	−2.792	−2.165
	(17.7007)	(18.1092)	(5.0707)	(4.8915)	(2.5514)	(2.4655)
Cons.	23.21 **	31.14 ***	24.47 ***	28.85 ***	20.89 ***	22.22 ***
	(9.3945)	(9.5861)	(5.0682)	(4.5467)	(2.4394)	(2.5981)
W-direct		−0.0259		−0.0206 *		−0.0114
		(0.0199)		(0.0110)		(0.0070)
W-speed		−2.485 ***		−0.376		0.270
		(0.8395)		(0.3486)		(0.3771)
Obs.	610	610	476	476	375	375
R^2	0.023	0.064	0.029	0.034	0.225	0.226
AIC	5981.5348	5957.6179	4351.1048	4350.8248	2777.9489	2779.5645
BIC	6016.8425	6001.7525	4376.0973	4384.1481	2809.3643	2818.8337
Order	9	9	2	2	9	9
	Jan-2-SO_2		**Feb-2-SO_2**		**Mar-2-SO_2**	
r	−1112.7 ***	−1008.2 ***	−1039.0	−1019.2	−124.9	−166.8
	(164.0574)	(170.8893)	(738.2869)	(731.1258)	(131.8672)	(130.0576)
Cons.	1282.0 ***	1044.0 ***	923.0 **	1173.0 **	414.5 ***	446.4 *
	(121.1226)	(236.3485)	(362.0540)	(467.9427)	(109.5450)	(251.3828)
W-direct		1.379		−0.0146		−0.673
		(0.8898)		(1.2270)		(0.8346)
W-speed		−10.04		−108.7 ***		63.84 **
		(16.8009)		(40.3243)		(25.0253)
Obs.	612	612	476	476	400	400
R^2	0.025	0.027	0.097	0.110	0.115	0.126
AIC	10523.1569	10524.0205	8044.7901	8038.1446	6584.2698	6581.2427
BIC	10540.8239	10550.5209	8098.9405	8096.4605	6600.2357	6605.1915
Order	1	1	9	9	1	1

Values in parentheses are the standard deviations corrected for autocorrelation and heteroscedasticity; *, **, and *** indicate significant values at 10, 5, and 1%, respectively. The regression models (a) and (b) were fitted without and with covariates, respectively. Cons. Represents the constant term. W-direct and W-speed represent the influences of wind direction and wind speed, respectively. Obs. Denotes sample size, while R^2 indicates goodness of fit. AIC represents the Akaike information criterion value, and BIC represents the Bayesian information criterion value. Order is the order of $f(x_t)$.

3.2. Contribution of Ship Emissions to NO_2 Concentration

The scatter plot in Figure 3 shows the fitting results of NO_2 concentrations at two monitoring points in January, February, and March. It is evident that there are significant breakpoints in the NO_2 concentrations depicted in Figure 3b,c,e,f. This indicates that ship emissions have a substantial impact on the NO_2 levels in the air around the wharf. In Figure 3a, although there are no apparent breakpoints, the fitted curve after the breakpoint exhibits a clear downward trend, suggesting that ship activities still influence the NO_2 concentration at the wharf. Additionally, Figure 3d also displays noticeable breakpoints; however, surprisingly, higher values are observed after these breakpoints. This could be attributed to two distinct outliers present in the data collected after these breakpoints due to environmental factors or measurement errors from equipment. Nevertheless, despite this observation, it is evident that NO_2 concentrations decrease around the wharf when there is no ship activity. Overall, ship emissions significantly contribute to elevated levels of NO_2 concentration in the air surrounding wharfs.

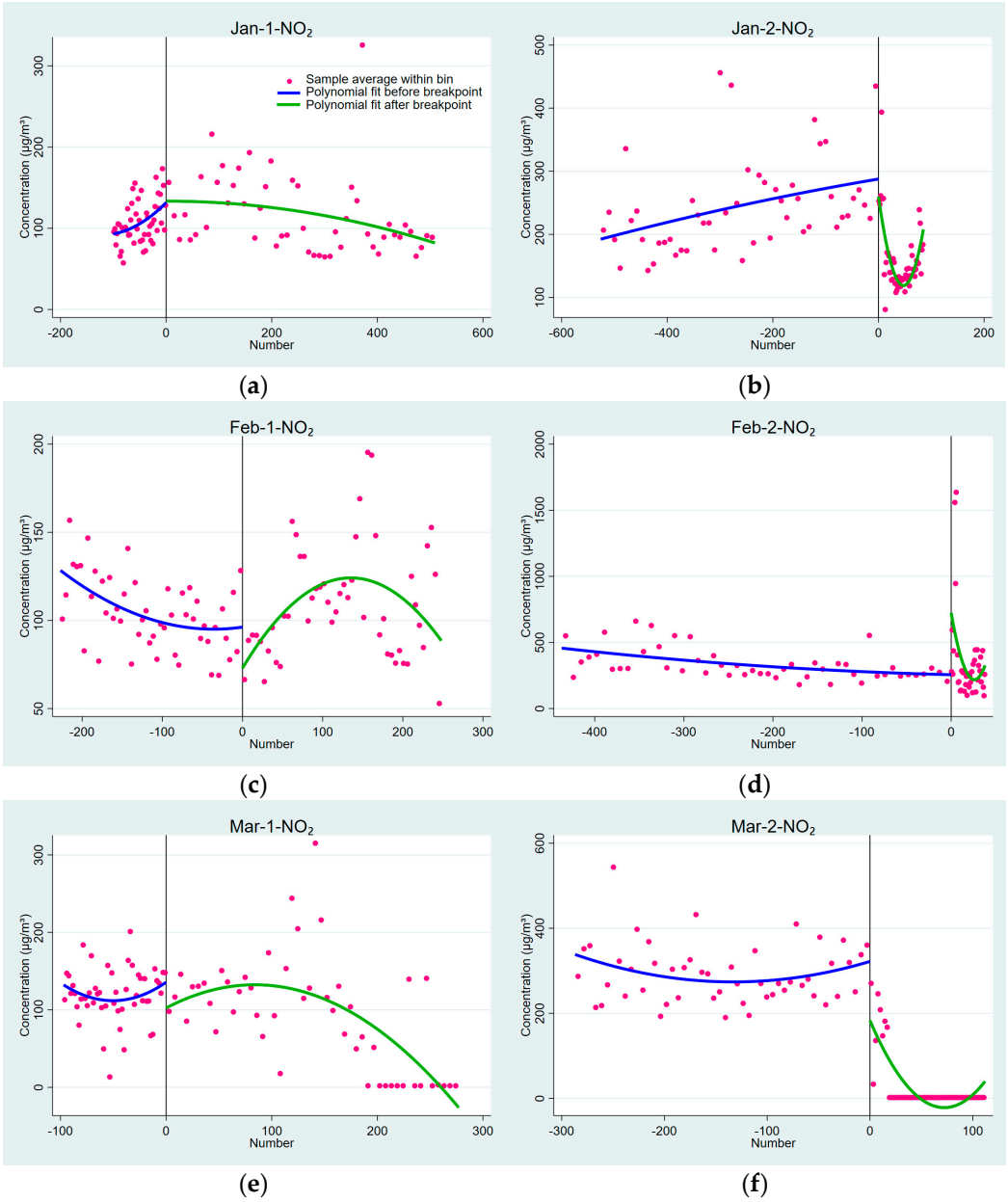

Figure 3. Hourly NO_2 concentrations for January, February, and March 2023 measured at the two monitoring stations of the Beilun wharf and their RD results.

The results of breakpoint regression quantification analysis are shown in Table 3. Group (a) represents the results without incorporating wind speed and direction control factors, while group (b) represents the results with these factors included. Among them, the estimated results for monitoring point 1 in February and March are significantly negatively correlated with monitoring point 2. After including the control variables, the estimated results are not significant but still negative. This result indicates that there is a noticeable change in NO_2 concentration when there is ship activity at the wharf compared to when there is no ship activity. The polynomial regression result of the second monitoring point in February is significantly negative, but the fitting diagram of the breakpoint shows an upward trend because different AIC values and BIC values will yield different fitting curves in the breakpoint's fitting diagram. In the fitting diagram of Feb-2-NO_2's breakpoint regression result, the BIC value corresponding to the order when the AIC value is minimum is not actually minimum. This discrepancy between the fitting result diagram and the regression result arises from selecting the r value associated

with the minimum AIC value in this study. The estimated result for monitoring point 1 in January, without including control variables, is 15.41; although it is positive, it is not significant. Considering the calculation results of the control variables, this may be partly due to wind speed causing interference on the sensors at the monitoring point, resulting in deviation of NO_2 concentration in wharf air. Further stability tests on the control variables need to be conducted in subsequent experiments. From the regression results, it can be observed that among the influencing factors of the control variables, wind speed shows a negative correlation with NO_2 concentration. This suggests that an increase in wind speed will decrease the average hourly NO_2 concentration at the wharf and introduce certain interference effects on policy implementation.

Table 3. Polynomial regression results of NO_2.

	Jan-1-NO_2		**Feb-1-NO_2**		**Mar-1-NO_2**	
	(a)	**(b)**	**(a)**	**(b)**	**(a)**	**(b)**
r	15.41	−2.503	−40.37 **	−18.13	−67.79 ***	−60.72 **
	(17.2224)	(15.7757)	(18.1622)	(17.4438)	(24.5960)	(23.4476)
Cons.	137.7 ***	146.8 ***	141.8 ***	128.4 ***	129.2 ***	142.2 ***
	(12.8295)	(10.8008)	(16.3041)	(15.6854)	(14.0936)	(16.0923)
W-direct		0.0981 ***		0.0964 ***		−0.0930
		(0.0214)		(0.0155)		(0.0565)
W-speed		−11.22 ***		−6.879 ***		−0.179
		(1.0504)		(1.0050)		(3.5119)
Obs.	610	610	476	476	375	375
R^2	0.162	0.319	0.240	0.343	0.260	0.261
AIC	6556.7985	6432.1928	4629.5417	4561.8532	4343.6122	4344.8338
BIC	6592.1062	6476.3274	4667.0305	4607.6728	4378.9545	4388.0300
Order	9	9	9	9	9	9
	Jan-2-NO_2		**Feb-2-NO_2**		**Mar-2-NO_2**	
r	−105.9 ***	−110.1 ***	−55.10 *	−135.7	−138.6 ***	−68.94
	(25.6175)	(26.6484)	(126.6651)	(144.7711)	(44.4093)	(139.6391)
Cons.	291.2 ***	398.3 ***	272.8 ***	196.2 *	322.0 ***	256.9 ***
	(17.8754)	(31.4622)	(74.3734)	(104.9382)	(26.2869)	(97.3885)
W-direct		−0.334 ***		0.743 *		0.256 *
		(0.1013)		(0.3925)		(0.1367)
W-speed		−14.72 ***		−37.16 ***		−20.18 ***
		(2.3567)		(11.1258)		(5.9190)
Obs.	612	612	476	476	400	400
R^2	0.054	0.106	0.054	0.093	0.392	0.411
AIC	7941.4128	7908.6692	6903.1777	6884.9722	5157.6357	5139.4242
BIC	7959.0798	7935.1695	6957.3282	6947.4535	5181.5845	5183.3303
Order	1	1	9	9	2	9

The abbreviations are the same as for Table 2.

3.3. Contribution of Ship Emissions to $PM_{2.5}$ Concentration

In Figure 4, it can be observed that both monitoring points exhibit breakpoints in the average $PM_{2.5}$ concentration, indicating significant differences in $PM_{2.5}$ levels in the air at the wharf with and without ship activities. The presence of numerous outliers within the samples has affected the direction and magnitude of the fitted curve for interval $PM_{2.5}$ values. Specifically, Figure 4a,b,d show clear upward breakpoints; however, scatter plots in the fitting graph are predominantly distributed between 0 and 100 $\mu g/m^3$, and post-breakpoint fitted curves tend to decrease, with some values being even lower than before the breakpoint. This suggests that although there is no significant reduction in mass concentration of $PM_{2.5}$ around the wharf before and after ship activities, it is still influenced by ship emissions.

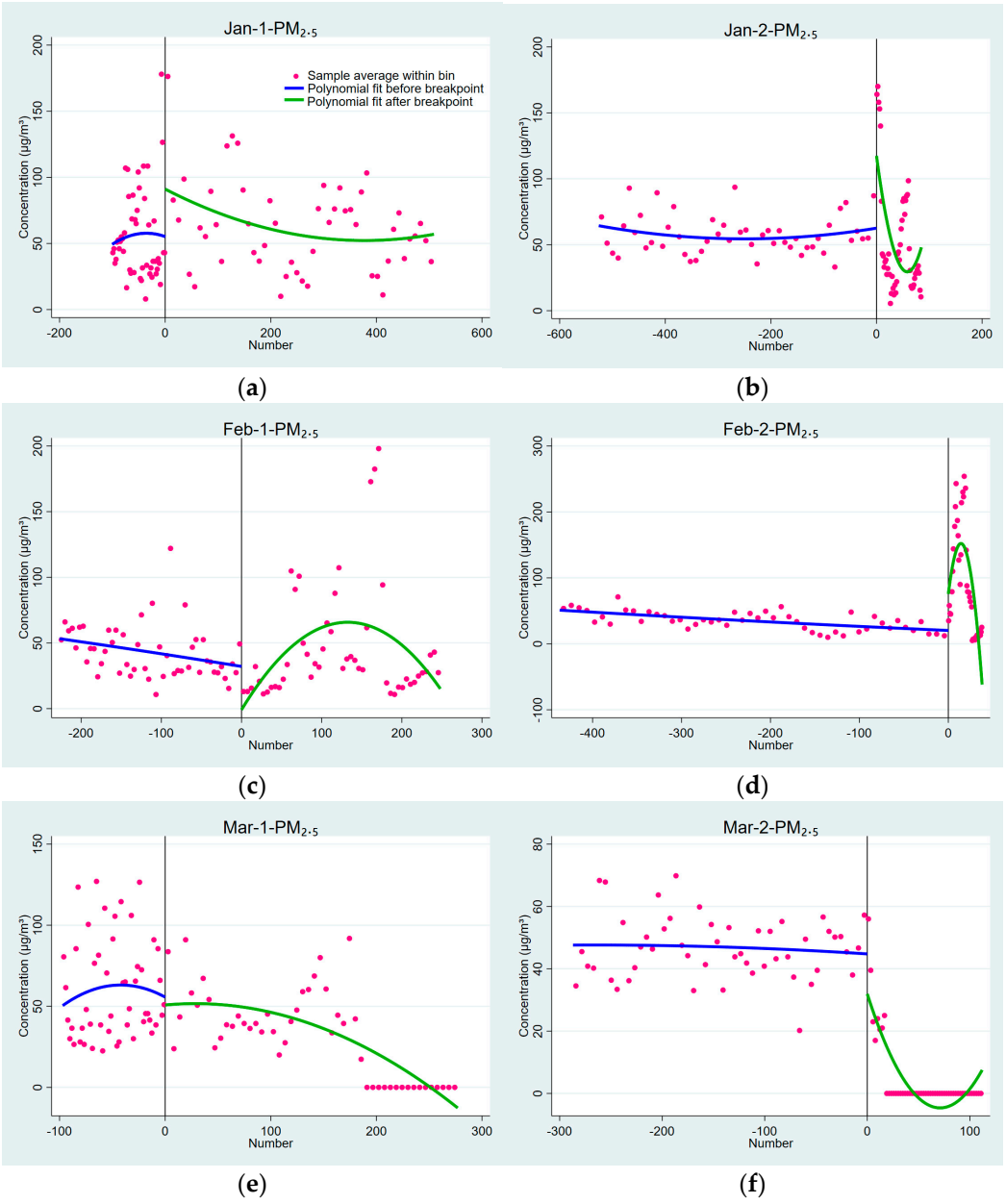

Figure 4. Hourly $PM_{2.5}$ concentrations for January, February, and March 2023 measured at the two monitoring points of the Beilun wharf and their RD results.

The regression analysis results of $PM_{2.5}$ are shown in Table 4, where (a) represents the results without considering wind speed and wind direction as control factors, and (b) represents the results with the inclusion of wind speed and wind direction as control factors. The correlation coefficient (*r* value) for monitoring points in Jan-1-$PM_{2.5}$, Feb-1-$PM_{2.5}$, and Feb-2-$PM_{2.5}$ shows a significant positive correlation. This corresponds to the preliminary test results presented in Figure 4, which show an upward breakpoint. However, the estimated result for monitoring point 1 in February shows a negative correlation, indicating that when there is ship activity at the wharf, the concentration of $PM_{2.5}$ in the air is significantly higher compared to when there is no ship activity. Based on quantitative analysis results, it can be observed that including control variables significantly reduces the estimated coefficients' impact at monitoring point 1 compared to not including them. Both wind direction and wind speed have positive impact estimates on $PM_{2.5}$ concentration at this point, indicating a positive correlation between wharf windspeed and average $PM_{2.5}$ concentration in its air. When there is downwind (west or southwest winds mainly ranging

from 180° to 270°), detected $PM_{2.5}$ concentrations tend to decrease due to lower influence from windspeed and direction interference caused by policy measures. On the other hand, monitoring point number two lies within an area with high ship activity density; hence, any effect from wharf's windspeed or wind direction on $PM_{2.5}$ concentration in its air would be relatively small.

Table 4. Polynomial regression results of $PM_{2.5}$.

	Jan-1-$PM_{2.5}$		**Feb-1-$PM_{2.5}$**		**Mar-1-$PM_{2.5}$**	
	(a)	**(b)**	**(a)**	**(b)**	**(a)**	**(b)**
r	145.8 ***	122.4 ***	−24.50	−30.25 **	3.229	−10.60
	(22.9480)	(20.4822)	(15.4778)	(13.9494)	(30.0205)	(24.8634)
Cons.	61.08 ***	39.00 **	68.16 ***	33.34 **	55.20 ***	31.76 ***
	(20.8383)	(17.5397)	(15.1040)	(13.8869)	(14.1616)	(10.2995)
W-direct		0.145 ***		0.133 ***		0.150 ***
		(0.0150)		(0.0180)		(0.0200)
W-speed		2.132 ***		2.926 ***		3.329 ***
		(0.5265)		(1.0331)		(1.0605)
Obs.	610	610	476	476	375	375
R2	0.383	0.545	0.217	0.344	0.457	0.592
AIC	5901.5872	5717.1799	4722.3069	4640.3390	3478.4248	3372.9327
BIC	5936.8949	5761.3145	4759.7957	4686.1586	3513.7671	3416.1288
Order	9	9	9	9	9	9
	Jan-2-$PM_{2.5}$		**Feb-2-$PM_{2.5}$**		**Mar-2-$PM_{2.5}$**	
r	76.74 ***	89.04 ***	41.71 *	45.31 *	2.800	5.897
	(20.0382)	(21.8726)	(22.9094)	(23.4297)	(16.3733)	(17.3511)
Cons.	89.92 ***	93.07 ***	14.00 **	20.27 **	59.40 ***	80.57 ***
	(18.1255)	(19.0162)	(5.5101)	(9.2260)	(12.9843)	(14.1172)
W-direct		−0.111 ***		−0.0311		−0.0854 ***
		(0.0205)		(0.0246)		(0.0211)
W-speed		3.044 ***		0.206		1.359
		(0.6019)		(0.9895)		(1.0168)
Obs.	612	612	476	476	400	400
R2	0.207	0.291	0.584	0.584	0.520	0.520
AIC	5975.1594	5910.4167	4381.5632	4383.5231	3523.6482	3523.6482
BIC	6023.7434	5972.2509	4431.5482	4441.8390	3579.5287	3579.5287
Order	9	9	9	9	9	9

The abbreviations are the same as for Table 2.

3.4. Contribution of Ship Emissions to PM_{10} Concentration

The scatter plots of PM_{10} concentration data are shown in Figure 5a–f. The fitting results for $PM_{2.5}$ concentration do not differ significantly as the diameter of PM emitted by ships is generally around PM_1, which aligns with previous monitoring results from actual ship emissions.

The regression results, as shown in Table 5, indicate the effects of including or excluding wind speed and direction control factors. The regression results for $PM_{2.5}$ concentration exhibit similar trends. For monitoring point 1, the inclusion of wind speed and direction control variables leads to a decrease in estimated coefficients, indicating a positive correlation between wind speed/direction and PM_{10} concentration at the port area. This aligns with real-world observations, suggesting that wind conditions at the port can influence PM_{10} levels to some extent. On the other hand, for monitoring point 2, the estimation results show that wind speed and direction have little impact on surrounding air quality. Overall, it can be concluded that ship activities do not strongly affect PM_{10} concentration variations in the port's air environment; however, implementation of ECA policies has had a slight effect on particle restrictions.

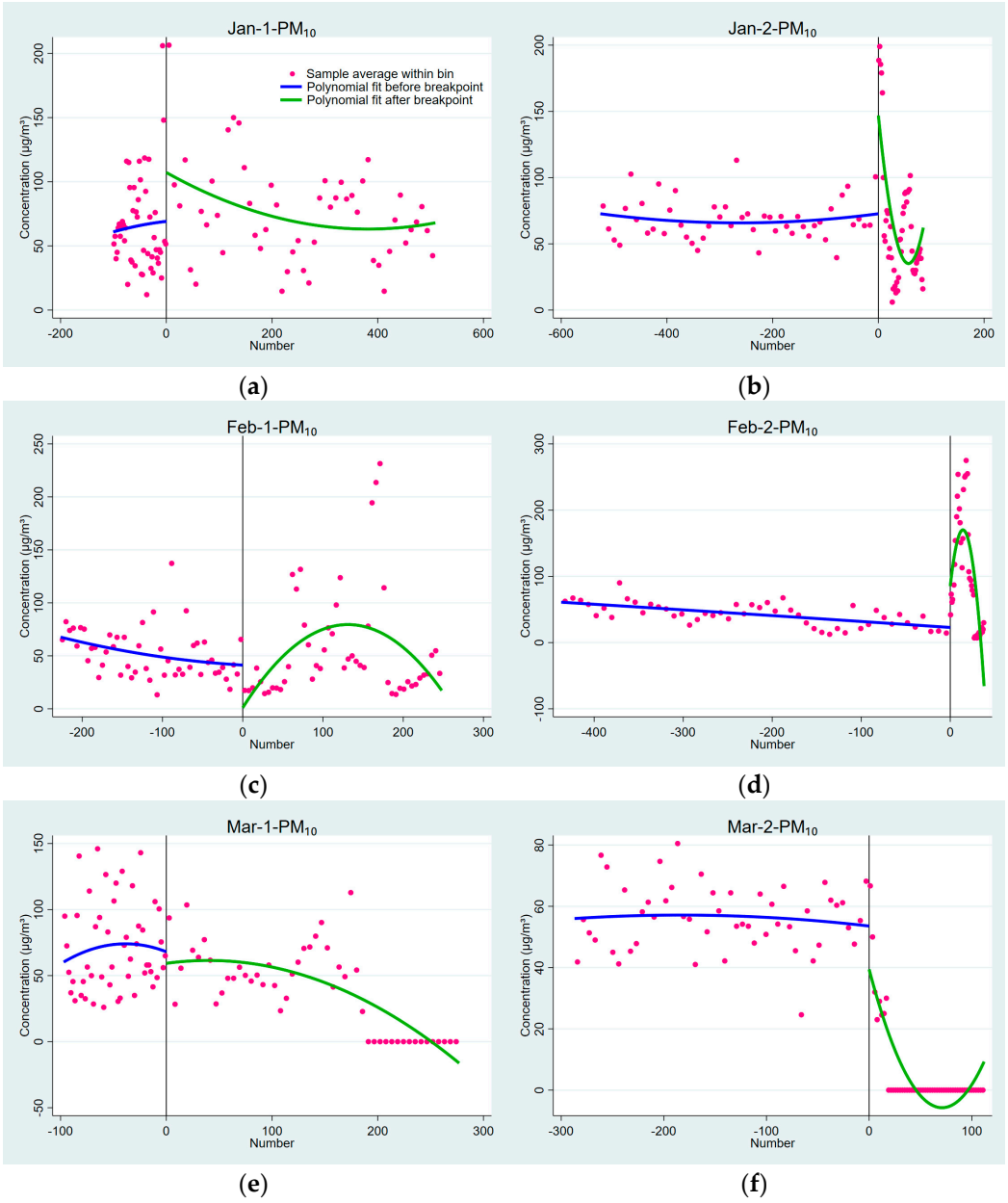

Figure 5. Hourly PM_{10} concentrations for January, February, and March 2023 measured at the two monitoring points of the Beilun wharf and their RD results.

Table 5. Polynomial regression results of PM_{10}.

	Jan-1-PM_{10}		**Feb-1-PM_{10}**		**Mar-1-PM_{10}**	
	(a)	**(b)**	**(a)**	**(b)**	**(a)**	**(b)**
r	165.0 ***	139.7 ***	−28.72	−34.45 *	−0.562	−15.98
	(26.2679)	(23.7836)	(20.8694)	(18.6786)	(32.9106)	(27.3660)
Cons.	75.60 ***	52.25 **	86.04 ***	45.37 **	67.64 ***	41.65 ***
	(23.7386)	(20.2866)	(20.6905)	(18.9740)	(15.2023)	(11.3769)
W-direct		0.157 ***		0.157 ***		0.165 ***
		(0.0173)		(0.0206)		(0.0220)
W-speed		2.027 ***		3.094 ***		3.896 ***
		(0.6057)		(1.1705)		(1.1666)
Obs.	610	610	476	476	375	375

Table 5. *Cont.*

	Jan-1-PM_{10}		Feb-1-PM_{10}		Mar-1-PM_{10}	
	(a)	**(b)**	**(a)**	**(b)**	**(a)**	**(b)**
R2	0.386	0.531	0.231	0.355	0.488	0.616
AIC	6033.7600	5871.6454	4867.2453	4785.4347	3557.1202	3451.0289
BIC	6069.0677	5915.7800	4904.7340	4831.2543	3592.4626	3494.2250
Order	9	9	9	9	9	9
	Jan-2-PM_{10}		**Feb-2-PM_{10}**		**Mar-2-PM_{10}**	
r	91.96 ***	156.4 ***	45.24 *	50.29 **	3.903	7.486
	(22.1721)	(13.7461)	(23.7854)	(24.8519)	(17.1823)	(17.8837)
Cons.	106.1 ***	81.49 ***	18.31 ***	29.15 ***	70.53 ***	93.23 ***
	(20.0962)	(9.3967)	(6.3158)	(10.6915)	(13.8841)	(15.2305)
W-direct		−0.107 ***		−0.0421		−0.0911 ***
		(0.0246)		(0.0295)		(0.0235)
W-speed		2.954 ***		−0.756		1.134
		(0.5653)		(1.1045)		(1.0790)
Obs.	612	612	476	476	400	400
R2	0.202	612	0.559	0.559	0.526	0.555
AIC	6086.6830	0.242	4525.7206	4525.7136	3627.7743	3602.3244
BIC	6135.2670	6061.3193	4579.8710	4584.0295	3667.6889	3646.2305
Order	9	3	9	9	9	9

The abbreviations are the same as for Table 2.

4. Robustness Tests

4.1. Polynomial Order Test

When the polynomial function $f(x_t)$ takes continuous different orders, if the estimation results of the breakpoint regression model remain consistent, this indicates that changing the form of the polynomial function does not affect the robustness of the breakpoint regression results. In the study of SO_2, NO_2, and particulate matter, only the results corresponding to minimum AIC or BIC were provided for selecting the optimal order of polynomial functions, without providing fitting results for all orders. This study evaluates the robustness of regression models by selecting fitting results when choosing an order with second minimum AIC or BIC and incorporating wind speed and wind direction as control variables. For SO_2, there is no difference between the polynomial regression order test and the results in Section 3.1 (Table 6), indicating that global polynomial regression yields stable results. The polynomial order test on the dataset shows that policy implementation effectively reduces SO_2 concentration during ship berthing and departure in all datasets. For NO_2 (Table 7), the result of the polynomial order test shows a negative correlation, which is not significantly different from estimated coefficients and results tested in Section 3, suggesting that polynomial order test holds true. The polynomial regression order test results of the dataset indicate that the concentration of NO_2 in ships significantly decreases during berthing, suggesting that effective control of SO_2 emissions has been achieved after entering the ECA. The concentration of SO_2 does not vary significantly when entering and leaving wharfs or docking at a pier, but there is no control over NO_2 until ships begin to regulate its emissions during berthing and departure, resulting in a strong change in NO_2 concentration. As for $PM_{2.5}$ and PM_{10} (Tables 8 and 9), the results of the polynomial order test show that there is no significant difference between the estimated coefficients of influence for a sub-minimum order and those selected in Section 3. In summary, from the perspective of polynomial order testing results, our breakpoint regression results are robust.

Table 6. Polynomial regression test results of SO_2.

	Jan-1-SO_2		**Feb-1-SO_2**		**Mar-1-SO_2**	
	(a)	**(b)**	**(a)**	**(b)**	**(a)**	**(b)**
r	2.773	7.282	−10.62 **	−2.103	−2.824	−2.041
	(15.6710)	(16.0302)	(4.3417)	(8.1437)	(2.5663)	(2.4371)
Cons.	31.83 ***	35.51 ***	36.17 ***	22.95 ***	22.73 ***	22.84 ***
	(9.4605)	(9.7983)	(4.6429)	(7.4002)	(2.2561)	(2.3146)
W-direct	−0.0162	−0.0230	−0.0230 **	−0.0204 *	−0.0109	−0.0109
	(0.0172)	(0.0192)	(0.0115)	(0.0123)	(0.0069)	(0.0070)
W-speed	−2.413 ***	−2.632 ***	−0.284	−0.459	0.243	0.184
	(0.8320)	(0.8903)	(0.3303)	(0.5338)	(0.3282)	(0.3873)
Obs.	610	610	476	476	375	375
Order	7	8	1	4	7	8
	Jan-2-SO_2		**Feb-2-SO_2**		**Mar-2-SO_2**	
r	−924.4 ***	−972.6 ***	−1338.0	−1706.8	−177.9	40.62
	(249.0654)	(310.5208)	(960.1964)	(1.2×10^3)	(187.6219)	(366.9013)
Cons.	933.9 ***	787.7 **	963.6 **	1119.8 **	562.9 *	75.89
	(301.4602)	(355.8400)	(404.1852)	(467.2127)	(288.8566)	(402.1538)
W-direct	1.365	1.307	0.161	0.123	−0.731	−0.696
	(0.8843)	(0.8923)	(1.2162)	(1.2247)	(0.8472)	(0.9011)
W-speed	−8.063	−3.315	−99.02 **	−98.39 **	60.50 **	41.06
	(18.6425)	(18.8445)	(39.7765)	(40.1291)	(26.8508)	(33.4134)
Obs.	612	612	476	476	400	400
Order	2	3	6	8	2	9

(a) and (b) represent different orders of the polynomial order test.

Table 7. Polynomial regression test results of NO_2.

	Jan-1-NO_2		**Feb-1-NO_2**		**Mar-1-NO_2**	
	(a)	**(b)**	**(a)**	**(b)**	**(a)**	**(b)**
r	−18.67	14.80	−17.74	25.10	−72.80 ***	−53.84 **
	(13.8847)	(12.5796)	(20.0583)	(22.9982)	(23.7523)	(22.6553)
Cons.	148.1 ***	142.3 ***	130.7 ***	81.11 ***	150.6 ***	137.6 ***
	(11.6884)	(10.0387)	(17.0626)	(18.9451)	(15.6883)	(16.9575)
W-direct	0.122 ***	0.0952 ***	0.104 ***	0.110 ***	−0.0880	−0.0859
	(0.0207)	(0.0210)	(0.0161)	(0.0164)	(0.0560)	(0.0564)
W-speed	−9.465 ***	−11.07 ***	−6.830 ***	−7.383 ***	−1.467	−1.749
	(0.9718)	(0.9947)	(1.0214)	(1.0186)	(2.9995)	(3.3148)
Obs.	610	610	476	476	375	375
Order	6	8	7	8	6	8
	Jan-2-NO_2		**Feb-2-NO_2**		**Mar-2-NO_2**	
r	−117.3 ***	−348.0 **	−223.4	−268.1	−181.3 ***	−110.5 **
	(40.9096)	(139.0026)	(206.2792)	(213.9444)	(30.7005)	(45.7304)
Cons.	407.3 ***	620.8 ***	148.3	185.9 *	228.4 ***	284.4 ***
	(41.5317)	(131.7552)	(93.5502)	(104.6282)	(44.1951)	(44.9921)
W-direct	−0.333 ***	−0.338 ***	0.754 *	0.770 *	0.268 *	0.223 *
	(0.1008)	(0.1032)	(0.3889)	(0.3924)	(0.1379)	(0.1349)
W-speed	−14.89 ***	−16.13 ***	−36.31 ***	−35.17 ***	−5.840	−10.42 **
	(2.5298)	(2.7878)	(12.4280)	(11.0873)	(4.8405)	(5.0331)
Obs.	612	612	476	476	400	400
Order	2	9	7	8	1	2

The abbreviations are the same as for Table 6.

Table 8. Polynomial regression test results of $PM_{2.5}$.

	Jan-1-$PM_{2.5}$		**Feb-1-$PM_{2.5}$**		**Mar-1-$PM_{2.5}$**	
	(a)	**(b)**	**(a)**	**(b)**	**(a)**	**(b)**
r	100.8 ***	124.5 ***	−31.90 *	−28.02 *	−11.21	−10.39
	(20.5541)	(19.7094)	(16.6318)	(16.8766)	(20.8962)	(23.7263)
Cons.	55.00 ***	38.45 **	15.85	34.48 **	37.01 ***	37.13 ***
	(19.4552)	(17.4241)	(15.2917)	(15.9310)	(11.2713)	(11.3151)
W-direct	0.158 ***	0.145 ***	0.142 ***	0.139 ***	0.152 ***	0.152 ***
	(0.0141)	(0.0148)	(0.0190)	(0.0184)	(0.0198)	(0.0198)
W-speed	3.098 ***	2.151 ***	2.416 **	2.971 ***	2.896 ***	2.835 ***
	(0.4666)	(0.5272)	(1.0627)	(1.0586)	(1.0546)	(1.0779)
Obs.	610	610	476	476	375	375
Order	6	8	6	7	7	8
	Jan-2-$PM_{2.5}$		**Feb-2-$PM_{2.5}$**		**Mar-2-$PM_{2.5}$**	
r	142.4 ***	111.9 ***	41.04 ***	20.95 *	1.433	3.296
	(16.0360)	(24.0053)	(11.8484)	(11.3821)	(11.7442)	(14.3786)
Cons.	78.78 ***	92.79 ***	1.468	18.39 *	72.41 ***	75.16 ***
	(9.9065)	(19.0098)	(9.3271)	(9.4276)	(9.0309)	(11.6266)
W-direct	−0.112 ***	−0.111 ***	−0.0331	−0.0263	−0.0833 ***	−0.0821 ***
	(0.0210)	(0.0206)	(0.0259)	(0.0250)	(0.0207)	(0.0206)
W-speed	3.430 ***	3.095 ***	0.0608	0.572	0.816	0.864
	(0.5636)	(0.6022)	(1.0396)	(1.0328)	(0.9567)	(0.9720)
Obs.	612	612	476	476	400	400
Order	4	8	7	8	5	7

The abbreviations are the same as for Table 6.

Table 9. Polynomial regression test results of PM_{10}.

	Jan-1-PM_{10}		**Feb-1-PM_{10}**		**Mar-1-PM_{10}**	
	(a)	**(b)**	**(a)**	**(b)**	**(a)**	**(b)**
r	116.2 ***	143.1 ***	−30.77	10.70	−17.45	−15.89
	(23.7935)	(22.8213)	(22.7261)	(25.9303)	(23.1221)	(26.1425)
Cons.	69.25 ***	51.37 **	45.63 **	−4.521	47.31 ***	47.55 ***
	(22.5355)	(20.1329)	(21.9495)	(22.4377)	(12.4163)	(12.4646)
W-direct	0.172 ***	0.157 ***	0.165 ***	0.171 ***	0.167 ***	0.167 ***
	(0.0163)	(0.0172)	(0.0211)	(0.0215)	(0.0218)	(0.0218)
W-speed	3.133 ***	2.057 ***	3.138 ***	2.555 **	3.510 ***	3.393 ***
	(0.5427)	(0.6092)	(1.2004)	(1.2100)	(1.1565)	(1.1805)
Obs.	610	610	476	476	375	375
Order	6	8	7	8	7	8
	Jan-2-PM_{10}		**Feb-2-PM_{10}**		**Mar-2-PM_{10}**	
r	158.5 ***	121.9 ***	53.22 ***	26.71 **	4.801	13.47
	(17.6520)	(27.1317)	(12.9471)	(12.1045)	(12.0979)	(17.7141)
Cons.	91.00 ***	111.6 ***	4.992	27.33 **	84.41 ***	79.48 ***
	(11.4785)	(21.2122)	(10.9066)	(10.8392)	(9.8411)	(15.7067)
W-direct	−0.111 ***	−0.109 ***	−0.0464	−0.0374	−0.0884 ***	−0.0879 ***
	(0.0251)	(0.0247)	(0.0309)	(0.0299)	(0.0231)	(0.0229)
W-speed	2.894 ***	2.479 ***	−1.077	−0.403	0.546	0.613
	(0.5879)	(0.6288)	(1.1508)	(1.1383)	(1.0105)	(1.0385)
Obs.	612	612	476	476	400	400
Order	4	8	7	8	5	8

The abbreviations are the same as for Table 6.

4.2. Local Linear Regression Test

The estimation results of the breakpoint regression model are not only influenced by the polynomial order but also by the bandwidth, which represents the sample size. In order

to ensure the robustness of the breakpoint regression analysis, this study refers to three different bandwidths using a triangular kernel function: optimal bandwidth, 0.5 times optimal bandwidth, and 2 times optimal bandwidth. The significant changes in SO_2, NO_2, $PM_{2.5}$, and PM_{10} concentrations in the local dataset near the breakpoints were analyzed to evaluate whether there are significant variations.

From the test results (Table 10), the concentration of SO_2 in the air at the wharf during ship activities does not show a significant upward or downward trend, indicating that the restrictions on SO_2 have been effective after ships enter emission control areas. The test results for NO_2 show a negative correlation under optimal bandwidth conditions, which is consistent with the evaluation and analysis findings mentioned earlier. Similarly, local linear regression results for $PM_{2.5}$ and PM_{10} concentrations align closely with those discussed in the analysis section in Chapter 3, suggesting that ECA policies have had moderate effects on average $PM_{2.5}$ concentration at port terminals for ship emissions control zones. Overall, considering all factors together, including optimum bandwidth outcomes compared to breakpoint regression results, our results indicate no significant differences, indicating the robustness of our findings.

Table 10. Local linear regression results.

	Jan-1-SO_2	**Jan-2-SO_2**	**Feb-1-SO_2**	**Feb-2-SO_2**	**Mar-1-SO_2**	**Mar-2-SO_2**
r-Treat	14.25	−1651.3 **	0.530	998.5	0.136	269.6
	(17.1136)	(607.6906)	(0.4156)	(723.3712)	(0.1909)	(194.2858)
r-0.5Treat	4.386	−1600.6	−0.00474	895.2	−0.152	−176.5
	(16.7375)	(899.2198)	(0.2832)	(815.5242)	(0.1728)	(176.2007)
r-2Treat	22.33	−1432.3 ***	2.280	892.4	−0.395	89.03
	(19.4037)	(394.3879)	(1.9783)	(570.0589)	(0.4656)	(143.2453)
Obs.	610	612	476	476	375	400
Bandwidth	14.171	51.522	16.920	31.733	12.221	36.257
0.5Bandwidth	7.085	25.761	8.460	15.866	6.110	18.129
2Bandwidth	28.342	103.044	33.840	63.465	24.441	72.515
	Jan-1-NO_2	**Jan-2-NO_2**	**Feb-1-NO_2**	**Feb-2-NO_2**	**Mar-1-NO_2**	**Mar-2-NO_2**
r-Treat	50.38 **	−171.3	−58.41 *	505.9 *	−82.27 **	−108.7
	(15.9598)	(128.2951)	(22.6910)	(203.3348)	(29.9077)	(91.8356)
r-0.5Treat	62.69 *	−114.7	−88.98 ***	373.0	−113.8 ***	−84.44
	(28.1420)	(106.4232)	(26.6140)	(200.9858)	(24.6000)	(129.7557)
r-2Treat	26.49 *	−133.3	−37.23 *	358.0 *	−44.38	−131.9 *
	(12.3482)	(105.3698)	(16.3412)	(157.3304)	(22.7000)	(58.4997)
Obs.	610	612	476	476	375	400
Bandwidth	20.517	29.940	17.011	26.299	15.446	28.328
0.5Bandwidth	10.259	14.970	8.505	13.149	7.723	14.164
2Bandwidth	41.035	59.880	34.022	52.598	30.891	56.657
	Jan-1-$PM_{2.5}$	**Jan-2-$PM_{2.5}$**	**Feb-1-$PM_{2.5}$**	**Feb-2-$PM_{2.5}$**	**Mar-1-$PM_{2.5}$**	**Mar-2-$PM_{2.5}$**
r-Treat	126.9 ***	96.03 **	−40.53	27.67 *	86.66 ***	−14.43
	(25.0367)	(30.8501)	(21.9873)	(11.9530)	(21.9778)	(13.0543)
r-0.5Treat	173.3 ***	99.84 ***	−43.57	8.818	124.4 ***	−19.40
	(32.2121)	(28.1322)	(37.5581)	(12.2649)	(24.7886)	(13.7465)
r-2Treat	106.9 ***	78.01 ***	−26.16 *	92.14 ***	19.66	−7.976
	(20.9531)	(20.7879)	(12.4798)	(23.2392)	(29.0283)	(10.7649)
Obs.	610	612	476	476	375	400
Bandwidth	20.675	16.370	18.985	15.979	12.388	15.263
0.5Bandwidth	10.337	8.185	9.492	7.989	6.194	7.631
2Bandwidth	41.350	32.741	37.970	31.959	27.777	30.526

Table 10. *Cont.*

	Jan-1-PM_{10}	Jan-2-PM_{10}	Feb-1-PM_{10}	Feb-2-PM_{10}	Mar-1-PM_{10}	Mar-2-PM_{10}
r-Treat	146.8 ***	104.7 **	−51.96	36.36 **	94.98 ***	−14.29
	(29.3011)	(32.8487)	(30.1596)	(11.5137)	(24.3994)	(13.5718)
r-0.5Treat	193.7 ***	101.1 **	−57.68	18.00	126.0 ***	−18.96
	(36.4751)	(33.7825)	(52.6159)	(11.9622)	(28.9203)	(13.9000)
r-2Treat	122.6 ***	88.39 ***	−31.60	103.0 ***	19.53	−7.130
	(23.6716)	(21.9854)	(17.0931)	(23.4678)	(32.0962)	(11.5271)
Obs.	610	612	476	476	375	400
Bandwidth	21.763	18.081	19.710	16.011	11.871	15.444
0.5Bandwidth	10.881	9.040	9.855	8.005	5.935	7.722
2Bandwidth	43.526	36.162	39.421	32.022	23.743	30.889

BW, 0.5BW, and 2BW represent the optimal bandwidth, half of the optimal bandwidth, and twice the optimal bandwidth, respectively. Treat, 0.5Treat, and 2Treat, respectively, represent the results of breakpoint regression analysis conducted with half and twice the optimal bandwidth.

4.3. Continuity Test for Covariates

Due to the influence of various factors on the concentration changes of SO_2, NO_2, $PM_{2.5}$, and PM_{10} in the air, this study will use a continuous test with controlled variables to eliminate interference from other factors. The results in the Table 11 show the polynomial regression results with controlled variables. Based on these regression results, it is possible that the collected data on SO_2, NO_2, $PM_{2.5}$, and PM_{10} concentrations at monitoring points may be affected by wind direction and wind speed during monitoring. Therefore, wind direction and wind speed were selected for polynomial regression tests. From the regression results of monitoring point 1, it can be observed that there is no absolute stability or significance in correlation between wind speed and wind direction after breakpoints with four gas concentrations in January and February. This indicates that wind speed and wind direction have little contribution to the data on gas concentrations after breakpoints. The estimation results for March show significant correlation between wind speed/wind direction and gas concentrations, indicating slight-to-moderate interference from these factors. Although some values show significant positive correlation, the test results exhibit similar patterns and trends as those obtained after incorporating wind direction and wind speed in Chapter 3's regression analysis. This demonstrates the robustness of our breakpoint regression results.

Table 11. Continuity test of covariates.

	Jan-1		Feb-1		Mar-1	
	W-direct	**W-speed**	**W-direct**	**W-speed**	**W-direct**	**W-speed**
r	148.5 ***	−0.169	−21.33	3.634 ***	74.43 *	0.810 *
	(45.2110)	(0.6409)	(49.0234)	(0.5222)	(43.5234)	(0.4788)
Cons.	128.2 ***	1.895 ***	233.1 ***	0.378	137.5 ***	0.856 ***
	(38.4517)	(0.4743)	(35.0157)	(0.4365)	(33.6363)	(0.3222)
Obs.	610	610	476	476	375	375
R^2	0.236	0.474	0.126	0.181	0.241	0.288
Order	8	9	9	7	9	9
	Jan-2		**Feb-2**		**Mar-2**	
	W-direct	**W-speed**	**W-direct**	**W-speed**	**W-direct**	**W-speed**
r	−11.01	−4.004 ***	105.0 ***	0.167	14.79	0.887
	(13.8597)	(1.3334)	(18.2675)	(0.7604)	(10.2252)	(1.0622)
Cons.	183.5 ***	4.754 ***	227.0 ***	2.270 ***	256.5 ***	0.371
	(8.0696)	(1.2721)	(8.2927)	(0.5891)	(5.7407)	(0.5517)
Obs.	612	612	476	476	400	400
R^2	0.078	0.389	0.149	0.229	0.096	0.322
Order	2	9	4	9	1	9

The abbreviations are the same as for Table 2.

5. Conclusions

The implementation of ship ECA policies has effectively improved the air quality in port areas. However, previous studies have mainly focused on changes in sulfur dioxide (SO_2) concentrations in the air, lacking monitoring and analysis of other major pollutants. This study is based on atmospheric measurement data for SO_2, NO_2, $PM_{2.5}$, and PM_{10} at Beilun wharf at China's Ningbo port. Using an RD model, we analyzed the impact of ship emissions on port air quality.

The analysis results for SO_2 indicate that ships near the monitoring points did not significantly affect the concentration of SO_2 in the air. This suggests that ship ECA policies have significantly limited ships' contribution to airborne SO_2 levels. However, due to China's current ECA policy not including restrictions on NO_x emissions, there was a significant increase in NO_2 concentration when ships approached the monitoring points, with a clear breakpoint observed in the RD model fitting results. Furthermore, ship emissions also led to variation in $PM_{2.5}$ and PM_{10} concentrations, respectively. These relatively small increments are because FSC restrictions indirectly reduce particle emissions and the characteristics of particulate matter emissions from ships.

Meanwhile, the results of the RD model have passed three robustness tests, indicating that the regression results of this study are reliable. Through a comparative analysis of these four pollutants, it was observed that wind speed and direction at monitoring points did not have a significant impact on SO_2 and NO_2 but showed a significant correlation with particle concentration. This is consistent with the weather conditions at that time and may be due to the interference of haze weather on port particle concentration levels in relation to ECA policy effects; even a shipwreck could have had an impact on air quality at the time [36]. Overall, the analysis results of this study validate the effectiveness of policies limiting ship fuel sulfur content and further restricting ship emissions. However, a further reduction in harmful ship emissions may require more regulatory measures focused on nitrogen oxide emissions.

Author Contributions: S.L. wrote the article and contributed to the experiments. F.Z. designed the study and analyzed the experimental data. All authors have read and agreed to the published version of the manuscript.

Funding: This research received no external funding.

Institutional Review Board Statement: Not applicable.

Informed Consent Statement: Not applicable.

Data Availability Statement: Please address requests to Fan Zhou (fanzhou_cv@163.com).

Acknowledgments: This research was supported by Shanghai High-level Local University Innovation Team (Maritime Safety and Technical Support).

Conflicts of Interest: The authors declare no conflicts of interest.

References

1. Liu, H.; Fu, M.; Jin, X.; Shang, Y.; Shindell, D.; Faluvegi, G.; Shindell, C.; He, K. Health and climate impacts of ocean-going vessels in East Asia. *Nat. Clim. Chang.* **2016**, *6*, 1037–1041. [CrossRef]
2. Tong, M.; Zhang, Y.; Zhang, H.; Chen, D.; Pei, C.; Guo, H.; Song, W.; Yang, X.; Wang, X. Contribution of ship emission to volatile organic compounds based on one-year monitoring at a coastal site in the Pearl River Delta region. *J. Geophys. Res. Atmos.* **2024**, *129*, e2023JD039999. [CrossRef]
3. Mohajan, H.K. Acid Rain is a Local Environment Pollution but Global Concern. *J. Anal. Methods Chem.* **2018**, *3*, 47–55.
4. Sofiev, M.; Winebrake, J.J.; Johansson, L.; Carr, E.W.; Prank, M.; Soares, J.; Vira, J.; Kouznetsov, R.; Jalkanen, J.P.; Corbett, J.J. Cleaner fuels for ships provide public health benefits with climate tradeoffs. *Nat. Commun.* **2018**, *9*, 406. [CrossRef] [PubMed]
5. Jonson, J.E.; Gauss, M.; Schulz, M.; Jalkanen, J.P.; Fagerli, H. Effects of global ship emissions on European air pollution levels. *Atmos. Chem. Phys.* **2020**, *20*, 11399–11422. [CrossRef]
6. MARPOL. *International Convention for the Prevention of Pollution from Ships*; 1973 as Modified by the Protocol of 1978–Annex VI: Prevention of Air Pollution from Ships; International Maritime Organization (IMO): London, UK, 1997.

7. International Maritime Organization (IMO): Sulphur Oxides (SOx) and Particulate Matter (PM)–Regulation 14. 2016. Available online: https://www.imo.org/en/OurWork/Environment/Pages/Sulphur-oxides-(SOx)-%E2%80%93-Regulation-14.aspx (accessed on 1 November 2022).
8. Xu, L.; Luo, Y.; Chen, J.; Zhou, S. Capacity prioritization allocation and credit financing option in shipping freight forwarding market. *Comput. Ind. Eng.* **2024**, *189*, 0360–8352. [CrossRef]
9. Roy, W.V.; Schallier, R.; Roozendael, B.V.; Scheldeman, K.; Nieuwenhove, A.V.; Maes, F. Airborne monitoring of compliance to sulfur emission regulations by ocean-going vessels in the Belgian North Sea area. *Atmos. Pollut. Res.* **2022**, *13*, 101445.
10. Roy, W.V.; Schallier, R.; Roozendael, B.V.; Scheldeman, K.; Nieuwenhove, A.V.; Maes, F. Airborne monitoring of compliance to Nox emission regulations from ocean-going vessels in the Belgian North Sea. *Atmos. Pollut. Res.* **2022**, *13*, 101518.
11. National Bureau of Statistics of China. China Statistical Yearbook. 2023. Available online: https://www.stats.gov.cn/ (accessed on 1 April 2024).
12. MOT. *Implementation of the Ship Emission Control Area in Pearl River Delta, the Yangtze River Delta and the Bohai Rim (Beijing–Tianjin–Hebei Area)*; Ministry of Transport: Beijing, China, 2015. Available online: http://www.gov.cn/xinwen/2015-12/04/content_5019932.htm (accessed on 1 November 2022).
13. Ministry of Transport. *Implementation Scheme of the Domestic Emission Control Areas for Atmospheric Pollution from Vessels*; Ministry of Transport: Beijing, China, 2018. Available online: https://www.msa.gov.cn/public/documents/document/mtex/mzm1/~edisp/20181219111335546.pdf (accessed on 1 November 2022).
14. Diamond, M.S. Detection of large-scale cloud microphysical changes within a major shipping corridor after implementation of the International Maritime Organization 2020 fuel sulfur regulations. *Atmos. Chem. Phys.* **2023**, *23*, 8259–8269. [CrossRef]
15. Scott, E. Darkening clouds after restrictions in maritime sulfur emissions. *Nat. Rev. Earth Environ.* **2023**, *4*, 680. [CrossRef]
16. Zhou, F.; Fan, Y.; Zou, J.; An, B. Ship emission monitoring sensor web for research and application. *Ocean Eng.* **2022**, *249*, 110980. [CrossRef]
17. Saxe, H.; Larsen, T. Air pollution from ships in three Danish ports. *Atmos. Environ.* **2004**, *38*, 4057–4067. [CrossRef]
18. Topic, T.; Murphy, A.J.; Pazouki, K. Rose Norman, Nox Emissions Control Area (NECA) scenario for ports in the North Adriatic Sea. *J. Environ. Manag.* **2023**, *344*, 0301–4797. [CrossRef] [PubMed]
19. Dragović, B.; Tzannatos, E.; Tselentis, V.; Meštrović, R.; Škurić, M. Ship emissions and their externalities in cruise ports. *Transp. Res. D Transp. Environ.* **2018**, *61 Part B*, 289–300. [CrossRef]
20. Xiao, G.; Yang, D.; Xu, L.; Li, J.; Jiang, Z. The Application of Artificial Intelligence Technology in Shipping: A Bibliometric Review. *J. Mar. Sci. Eng.* **2024**, *12*, 624. [CrossRef]
21. Müller, T.; Shaikh, M. Your retirement and my health behavior: Evidence on retirement externalities from a fuzzy regression discontinuity design. *J. Health Econ.* **2018**, *57*, 45–59. [CrossRef] [PubMed]
22. Wan, Z.; Zhou, X.; Zhang, Q.; Chen, J. Do ship emission control areas in China reduce sulfur dioxide concentrations in local air? A study on causal effect using the difference-in-difference model. *Mar. Pollut. Bull.* **2019**, *149*, 110506. [CrossRef] [PubMed]
23. Zhang, Q.; Zheng, Z.; Wan, Z.; Zheng, S. Does emission control area policy reduce sulfur dioxides concentration in Shanghai? *Transp. Res. D Transp. Environ.* **2020**, *81*, 102289. [CrossRef]
24. Zhou, F.; Fan, Y.L. Determination of the Influence of Fuel Switching Regulation on the Sulfur Dioxide Content of Air in a Port Area Using DID Model. *Adv. Meteorol.* **2021**, 6679682. [CrossRef]
25. Zhang, Q.; Liu, H.; Wan, Z. Evaluation on the effectiveness of ship emission control area policy: Heterogeneity detection with the regression discontinuity method. *Environ. Impact Asses. Rev.* **2022**, *94*, 106747. [CrossRef]
26. Zhou, F.; Wang, Y.; Liu, J.; Yang, X.; Hu, Z.; Guo, T.; Zhu, H.; Han, Y. Influence of ship emission control area policy on air quality at Shanghai Port—Local and regional perspectives. *Ecol. Indic.* **2023**, *155*, 110951. [CrossRef]
27. Cullinane, K.; Bergqvist, R. Emission control areas and their impact on maritime transport. *Transp. Res. D-Tr. E.* **2014**, *28*, 1–5. [CrossRef]
28. Wu, Z.F.; Zhang, Y.; He, J.; Chen, H.; Huang, X.; Wang, Y.; Yu, X.; Yang, W.; Zhang, R.; Zhu, M.; et al. Dramatic increase in reactive volatile organic compound (VOC) emissions from ships at berth after implementing the fuel switch policy in the Pearl River Delta Emission Control Area. *Atmos. Chem. Phys.* **2020**, *20*, 1887–1900. [CrossRef]
29. Ningbo Municipal Statistics Bureau of China. Ningbo Statistical Yearbook. 2023. Available online: http://tjj.ningbo.gov.cn/ (accessed on 1 April 2024).
30. Zhang, Z.; Zheng, W.; Li, Y.; Cao, K.; Xie, M.; Wu, P. Monitoring Sulfur Content in Marine Fuel Oil Using Ultraviolet Imaging Technology. *Atmosphere* **2021**, *12*, 1182. [CrossRef]
31. Ma, Z.; Yang, Y.; Sun, P.; Xing, H.; Duan, S.; Qu, H.; Zou, Y. Analysis of Marine Diesel Engine Emission Characteristics of Different Power Ranges in China. *Atmosphere* **2021**, *12*, 1108. [CrossRef]
32. Zhou, F.; Liu, J.; Zhu, H.; Yang, X.; Fan, Y. A Real-Time Measurement- Modeling System for Ship Air Pollution Emission Factors. *J. Mar. Sci. Eng.* **2022**, *10*, 760. [CrossRef]
33. Zhou, F.; Pan, S.; Chen, W.; Ni, X.; An, B. Monitoring of compliance with fuel sulfur content regulations through unmanned aerial vehicle (UAV) measurements of ship emissions. *Atmos. Meas. Tech.* **2019**, *12*, 6113–6124. [CrossRef]
34. Wang, Q.; Jiang, M. Study on Emission Control of Berthing Vessels-Based on Non-Cooperative Game Theory. *Sustainability* **2023**, *15*, 10572. [CrossRef]

35. Amorim, P.; Parragh, S.N.; Sperandio, F.; Almada-Lobo, B. A rich vehicle routing problem dealing with perishable food: A case study. *Top* **2014**, *22*, 489–508. [CrossRef]
36. Chen, X.; Liu, S.; Liu, R.W.; Wu, H.; Han, B.; Zhao, J. Quantifying Arctic oil spilling event risk by integrating an analytic network process and a fuzzy comprehensive evaluation model. *Ocean Coast. Manag.* **2022**, *228*, 106326. [CrossRef]